9732 *Biochemistry* **2010,** *49,* 9732–9738
DOI: 10.1021/bi101029g

BIOCHEMISTRY
including biophysical chemistry & molecular biology
Article

Single-Molecule Study of Viomycin's Inhibition Mechanism on Ribosome Translocation†

Cindy T. Ly, Mediha E. Altuntop, and Yuhong Wang*

Department of Biology and Biochemistry, University of Houston, 4800 Calhoun Road, Houston, Texas 77214, United States

Received June 28, 2010; Revised Manuscript Received September 23, 2010

ABSTRACT: Viomycin belongs to the tuberactinomycin family of antibiotics against tuberculosis. However, its inhibition mechanism remains elusive. Although it is clear that viomycin inhibits the ribosome intersubunit ratcheting, there are contradictory reports about whether the antibiotic viomycin stabilizes the tRNA hybrid or classical state. By using a single-molecule FRET method to directly observe the tRNA dynamics relative to ribosomal protein L27, we have found that viomycin trapped the hybrid state within certain ribosome subgroups but did not significantly suppress the tRNA dynamics. The persistent fluctuation of tRNA implied that tRNA motions were decoupled from the ribosome intersubunit ratcheting. Viomycin also promoted peptidyl-tRNA fluctuation in the posttranslocation complex, implying that, in addition to acylated P-site tRNA, the decoding center also played an important role of ribosome locking after translocation. Therefore, viomycin inhibits translocation by trapping the hybrid state in the pretranslocation complex and disturbing the stability of posttranslocation complex. Our results imply that ribosome translocation is possibly a synergistic process of multiple decoupled local dynamics.

During protein biosynthesis, the ribosome moves along the mRNA template every three nucleotides while using amino acid-charged tRNA as the substrate to elongate polypeptide chains. There are three tRNA binding sites inside both of the ribosome 30S and 50S subunits: the A-, P-, and E-sites (*1*, *2*). During the translocation process, P/P and A/A tRNAs move to the E/E and P/P sites via the putative P/E and A/P hybrid states (*3*, *4*) (the first and second letters refer to the tRNA binding sites at the 30S and 50S subunits, respectively). The terms "pretranslocation"[1] and "posttranslocation" complexes refer to ribosome prior to and after this process. This stepwise model was first proposed in theory (*5*) and confirmed by detecting the chemical "footprinting" of tRNA binding sites inside ribosome (*3*). Further biochemistry studies supported the biological relevance of this finding (*4*, *6*−*9*).

The formation of the tRNA hybrid state is closely related to ribosome intersubunit ratcheting. Cryo-EM studies revealed a counterclockwise rotation of the 30S subunit relative to the 50S subunit either upon EF-G binding (*10*, *11*) or spontaneously (*12*, *13*). Prior to this ratcheting process, P-site tRNA was deacylated via peptidyl transferase reaction to "unlock" the ribosome. After translocation, the newly elongated peptidyl-tRNA moved from A-site into P-site to "lock" the ribosome into stable conformation (*10*). The combination of FRET and chemical footprinting studies on viomycin-trapped ribosome complexes indicated that the ratcheted-ribosome complex was identical to the tRNA hybrid state (*14*). These observations then implied that the tRNA movement to the hybrid state was coupled with ribosomal intersubunit rotation (*11*, *15*, *16*). However, direct dynamic study to test this hypothesis is scarce (*17*).

Viomycin belongs to the tuberactinomycin family of antibiotics, which inhibit ribosome translocation (*18*, *19*) by interacting with both the 30S and 50S ribosome subunits (*20*). The inhibition mechanism remains elusive regardless of tuberactinomycins as the most effective antibiotics against multidrug-resistant tuberculosis. A recent X-ray structural study showed that viomycin was bound to the classical state ribosome at the interface between helix 44 and helix 69 (*21*). Since this region may not change during intersubunit ratcheting, this result could not clarify whether viomycin also stabilized the tRNA P/E-A/P hybrid state. Contradictory conclusions were obtained from several studies regarding this issue. Single-molecule and ensemble FRET studies directly probing the intersubunit ratcheting yielded results that viomycin trapped the ratcheted state (*14*, *22*). However, another single-molecule FRET study probing tRNA−tRNA distances suggested that viomycin favored the tRNA classical state (*23*) while a more recent similar single-molecule FRET study observed a net stabilization of the hybrid state (*24*). On the other hand, a stopped-flow study of fluorescently labeled tRNA suggested that viomycin trapped the ribosome at a new "P/E-A/A" hybrid state wherein the P-site tRNA was in the P/E state and the A-site tRNA was in the classical state (*9*). These discrepancies implied that the intersubunit ratcheting and tRNA movement may be decoupled, contrary to previous conclusions (*11*, *14*, *25*). Furthermore, the stochastic nature of local ribosomal dynamics and their sensitivity to the experimental conditions and detection methods created additional ambiguity.

We reported that the ribosome dynamics were hierarchically arranged at the peptidyl transferase center (*26*). As shown in Figure 1, three well-defined FRET states with respective efficiencies of 0.2, 0.44, and 0.63 between A-site tRNA and ribosomal L27 protein were observed in the pretranslocation complex. But in

†This work is supported by start-up funds from the University of Houston and a grant to Y.W. from the Welch Foundation (E-1721).

*To whom correspondence should be addressed. E-mail: ywang60@uh.edu. Phone: 713-743-7941. Fax: 713-743-8651.

[1]Abbreviations: FRET, fluorescence resonance energy transfer; HaMMy, hidden Markov model analysis package; pretranslocation, ribosome conformation before the translocation process; posttranslocation, ribosome conformation after the translocation process; F-High, fluctuating ribosomes that sample 0.2/0.44/0.63 FRET states; F-Low, fluctuating ribosomes that sample only 0.2/0.44 FRET states; NF-High, nonfluctuating ribosomes that remain at 0.63 FRET state; NF-Low, nonfluctuating ribosomes that remain at 0.2 or 0.44 FRET states.

 Published on Web 10/01/2010

single ribosome traces, the sampling and fluctuation among these FRET states were distinguished and sorted into four different subgroups. For example, F-High ribosome subpopulation fluctuated among all three FRET states, F-Low subpopulation only fluctuated between 0.2 and 0.44 FRET states, NF-Low subpopulation was mainly static at 0.44 state, and NF-High subpopulation was static at 0.63 state. These observations indicated that tRNA dynamics inside the ribosome were regulated by a hierarchic mechanism in which the ribosome subpopulations dictated the sampling and fluctuation of FRET states, while specific FRET states did not represent specific ribosome subpopulations except in the static cases. In other words, the FRET states were at lower leveled dynamics compared to the ribosome subpopulations.

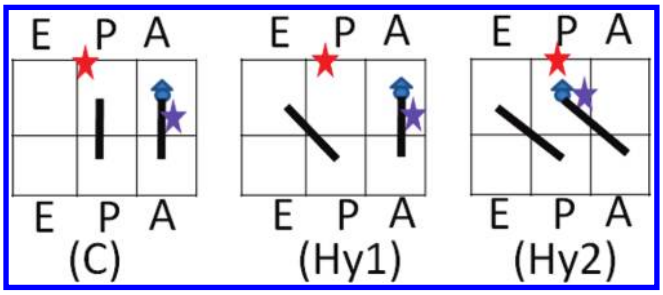

FIGURE 1: The tRNA configurations in the pretranslocation complex deduced from the A-site-labeled tRNA experiments. In these experiments, the ribosomal protein L27 is labeled with Cy5 and Phe-tRNA at the A-site is labeled with Cy3 dyes. The labeled complex in the context of X-ray structure is shown in Supporting Information Figure S1.

We here report a study of the viomycin inhibition mechanism by detecting the same FRET signal between the tRNA and the L27 protein at the peptidyl center. We observed similar subpopulation heterogeneity in the pretranslocation complex programmed with 032 mRNA, which coded for fMet-Phe-Lys as the first three amino acids. Binding of viomycin to this complex prompted the F-High subpopulation in both the pre- and posttranslocation complexes, while this effect was reversible in the posttranslocation complex. These results suggest (a) viomycin

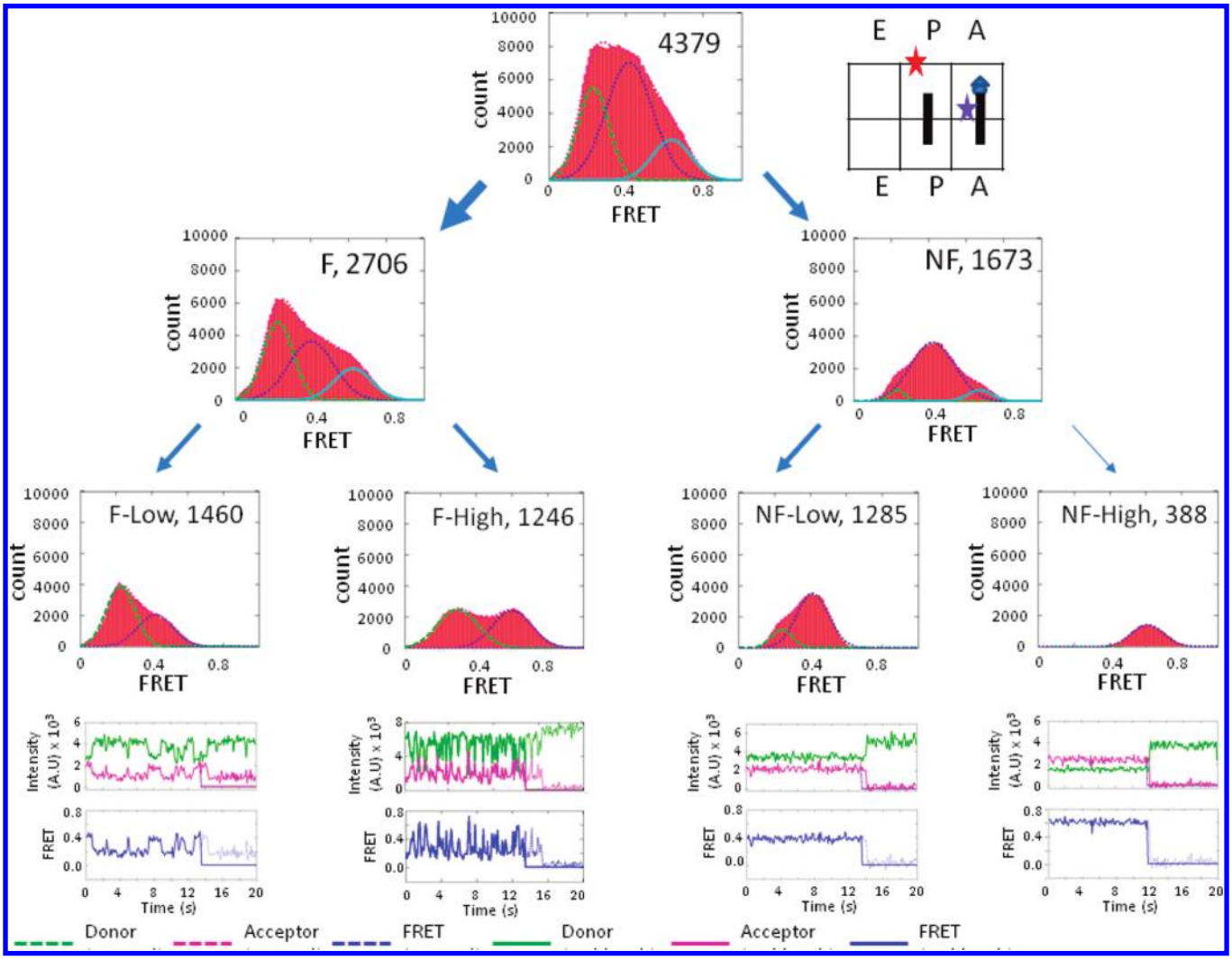

FIGURE 2: Histograms of the pretranslocation complex programmed with 032 mRNA coding for fMet-Phe-Lys.... Four horizontally arranged plots are shown. The top-tier plots show the FRET histogram of all of the ribosomes (4379 particles, as shown in parentheses) and the structure of the precomplex. The second-tier plots show the FRET histograms of the ribosomes separated into fluctuating (F, 2706 particles) and nonfluctuating (NF, 1673 particles) states. The third-tier plots show the FRET histograms of the ribosomes further separated into fluctuating below/above a FRET value of 0.6 (F-Low, 1460 particles/F-High, 1246 particles). Similar thresholds were applied to the NF-ribosomes to separate them into stable FRET states below/above 0.6 (NF-Low, 1285 particles/NF-High, 388 particles). The fourth-tier plots indicate the representative fluorescence traces of donor and acceptor species and the corresponding FRET traces (both the original and the truncated data) from each of the four subpopulations. Legends are shown in the plot.

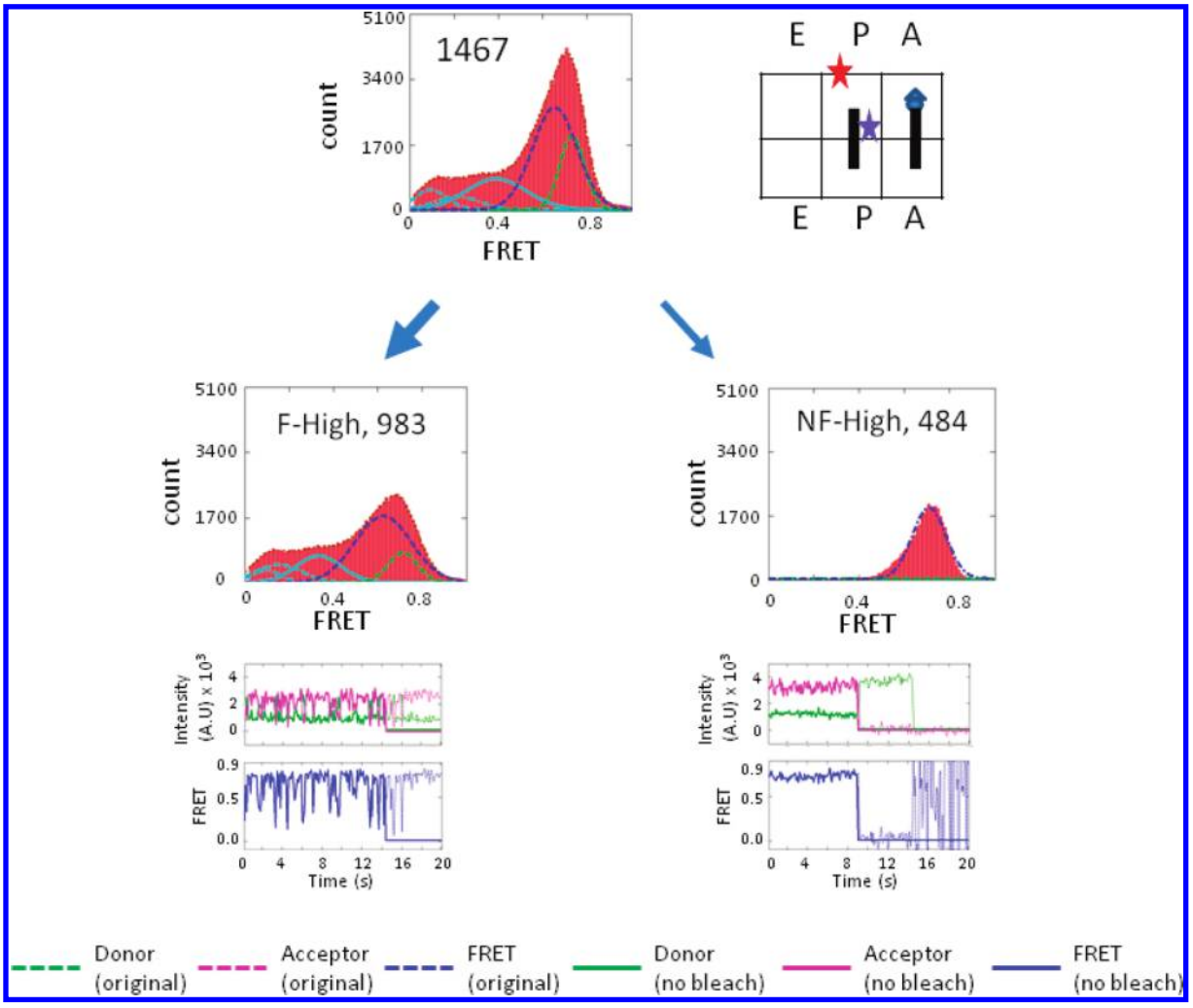

FIGURE 3: Histograms of the same pretranslocation complex in Figure 2 except the labeling position was at P-site fMet-tRNA not A-site Phe-tRNA. Only F-High (983 particles) and NF-High (484 particles) subpopulations were observed in significant amount.

inhibited the translocation by trapping the ribosome's F-High subpopulation and destabilizing the peptidyl-tRNA-locked post-translocation complex and (b) the tRNA movements were uncoupled from the ribosome intersubunit ratcheting.

EXPERIMENTAL PROCEDURES

Preparation of the ribosome labeled at the L27 protein C53 position, tRNAs labeled at the D16/17 position, and His-tagged initiation and elongation factors was described previously (*26*). The ribosome complexes were prepared similarly except that the poly(U) mRNA was replaced with 032 mRNA which included a strong Shine−Dalgarno sequence and AUG starting code followed by codons of phenylalanine and lysine. The A-site-labeled pretranslocation complex was generated by enzymatic delivery of the charged Phe-tRNA^{Cy3}·Tu·GTP ternary complex into the 032 mRNA-programmed ribosome initiation complex labeled at the L27 protein. For the P-site-labeled complex, charged-formylated fMet-tRNA^{Cy3} was used in ribosome initiation (Supporting Information Figure S1). Viomycin was incubated with the corresponding preformed complexes at 37 °C for 5 min in an Eppendorf tube or 10 min on the coverslip surface. All of the single-molecule data were collected using TAM_{10} buffer (20 mM Tris, pH 7.5, 30 mM NH_4Cl, 70 mM KCl, 10 mM $MgCl_2$, and 1 mM DTT) at room temperature and using an objective-based total internal reflection fluorescence microscope. The imaging buffer also included an oxygen-scavenging cocktail made of 3 mg/mL glucose, 100 μg/mL glucose oxidase, 48 μg/mL catalase, and 2 mM trolox (*27*, *28*). In the viomycin experiments, the same concentration of viomycin used during the incubation was also added in the final wash and during the imaging process. Data were collected at 100 ms intervals.

RESULTS

The tRNA Motions at both A- and P-Sites Indicated the Inhomogeneity in the Pretranslocation Complex. Figure 2 showed the ribosome subpopulations in the pretranslocation complex: "F-Low subpopulation" refers to the 1460 particles fluctuating only between the classical (C) and hybrid-1 (Hy1) states; "F-High subpopulation" refers to the 1246 particles fluctuating among C, Hy1, and hybrid-2 (Hy2) states; "NF-Low subpopulation" refers to 1285 particles consisting of 907 in the C state and 378 in the Hy1 state; and "NF-High subpopulation" refers to the 388 particles in the posttranslocation state due to spontaneous translocation. For the static subpopulations, the global conformations were the same as the FRET states. For the fluctuating subpopulations, the diversity of dynamics was due to the different ribosome global conformations (*26*). Although the FRET efficiency histogram of F-High subpopulation was fitted with two apparent FRET states in Figure 2, hidden Markov model analysis (*29*) and visional inspection of individual traces indicated

that 0.44 FRET state was probably involved. Only 106 out of the 1246 ribosome particles fluctuated between 0.2 and 0.63 FRET states exclusively. The remaining 91.5% ribosomes sampled the 0.44 FRET states with significant amount. Five representative traces from ribosomes sampling only two states (Supporting Information Figure S2a) or three states (Supporting Information Figure S2b) are shown in Supporting Information Figure S2.

The inhomogeneity was further studied via P-site tRNA motions in the similar pretranslocation complex (Figure 3). In these experiments, only F-High and NF-High were detected with significant amount. NF-High could be unambiguously assigned as the classical state (C) because P/P configuration was only compatible with A/A tRNA. We have assigned F-High as ribosomes with fluctuating P/E tRNA and A/A (or A/P) tRNA. This subpopulation had a very broad FRET distribution at the lower FRET values that was fitted with several Gaussian peaks (Figure 3). This broad distribution was probably due to weak ribosome−tRNA interaction at E-site (*2*), tRNA dynamic interaction with the L1 protein (*17*, *30*), and possible effect from the A-site tRNA fluctuation. Structurally, the distance between P and E sites is much larger than that between A and P sites in the 50S. Therefore, more complicated FRET efficiencies may exist for P/E fluctuation. We have chosen not to deconvolute the multiple P/E substates in order to keep our main arguments precise. Nevertheless, this simplified analysis agreed qualitatively with A-site-labeling experiments. Figure 4 showed the correlations

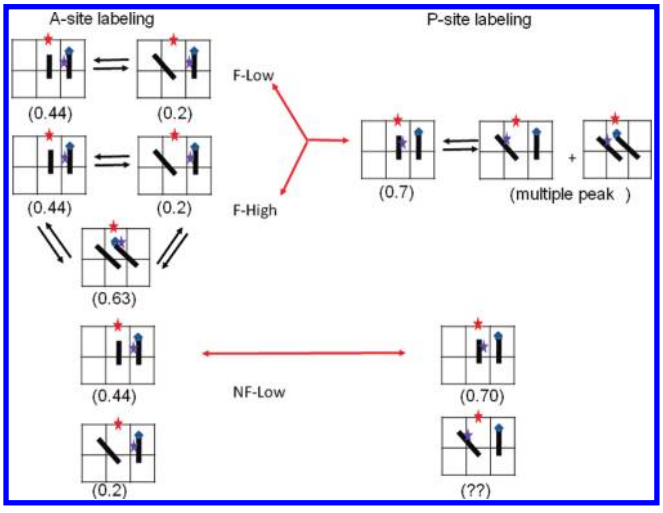

FIGURE 4: Ribosome subpopulations and FRET states detected from both the A- and P-site labeling. The red arrows indicate the correlation of identical complexes from the two labeling strategies.

of the ribosome subpopulations and the FRET states from the two labeling strategies. As indicated in both Figure 4 and Table 1, the sum of F-Low and F-High subpopulations in the A-site-labeling experiments corresponded to the F-High subpopulation in the P-site-labeling experiments. Meanwhile, the NF-Low subpopulation in the A-site-labeling experiments corresponded to NF-High subpopulation in the P-site-labeling experiments. Because A- and P-site tRNAs were Phe- and fMet- tRNAs, respectively, the FRET values varied slightly. These results supported our original assignment of the FRET states and the subpopulations (*26*). It seemed that we could not account for the small amount of stable Hy1 state (~6%) in the P-site-labeling experiments probably due to the very broad peaks with lower FRET efficiencies in these experiments.

Viomycin Decreased the F-Low and Increased the F-High Subpopulations in the Pretranslocation Complex and Inhibited EF-G Function. The interaction of viomycin with the pretranslocation complex was studied at three concentrations of viomycin: 5 μM (Supporting Information Figure S3), 100 μM (Figure 5), and 1 mM (Supporting Information Figure S4). Figure 5 shows the detailed FRET efficiency histogram in the presence of 100 μM viomycin. With increasing amount of viomycin, more F-High ribosome subpopulation was induced (Figure 6). Furthermore, Figure 6 showed that the F-High subpopulation increased at the expense of the F-Low subpopulation within the fluctuating species. However, it appeared not to affect the nonfluctuating ribosomes. The percentages of the NF-Low and NF-High ribosomes remained at relatively stable levels (Figure 6). This result was confirmed by adding viomycin into a pretranslocation complex labeled at the P-site fMet-tRNA. At this labeling position, F-Low and F-High populations were not distinguishable. Accordingly, we did not observe significant changes of the subpopulation distributions.

Incubating the viomycin-bound pretranslocation complex with EF-G·GTP did not form the posttranslocation complex (697 particles; data not shown). This agrees with the previous study showing that viomycin inhibits translocation (*7*, *18*).

Viomycin Induced More F-High Subpopulation and Stabilized the Hy2 State and Destabilized the Hy1 State in This Subpopulation. In the presence of 100 μM viomycin, the F-High subpopulation increased its population while apparently losing its ability to translocate. Kinetics analysis in Table 2 and Supporting Information Figure S5 showed the transitions among the FRET states based on the idealized traces from the hidden Markov model analysis package (HaMMy program) (*29*). In F-High subpopulations, the binding of viomycin decelerated the

Table 1[a]

A-site labeled			P-site labeled		
ribosome subpopulation	FRET state transitions	percentage	ribosome subpopulation	FRET state transitions	percentage
F-Low	Hy1 ⇔ C (0.2) ⇔ (0.44)	37 ± 5	F-High	(Hy1 + Hy2) ⇔ C	67 ± 4
F-High	(C + Hy1) ⇔ Hy2 (0.2 + 0.44) ⇔ (0.63)	31 ± 4		(0.1−0.3) ⇔ 0.7	
NF-Low	C (0.44)	26 ± 3	NF-High	C (0.7)	33 ± 5
	Hy1 (0.2)	6 ± 3	NF-Low	N/A	

[a]The pretranslocation ribosome subpopulations and FRET states detected from tRNAs at either the A- or P-site. The corresponding tRNA configurations are shown in Figure 4. The percentages of the corresponding subpopulations from the two different labeling sites agreed with each other, which supported our assignment of the FRET states. The spontaneously formed posttranslocation complex under the A-site labeling condition was eliminated from the analysis, while under the P-site labeling condition, the unstable E-site bound tRNA prevented us to detect a well-defined NF-Low subpopulation.

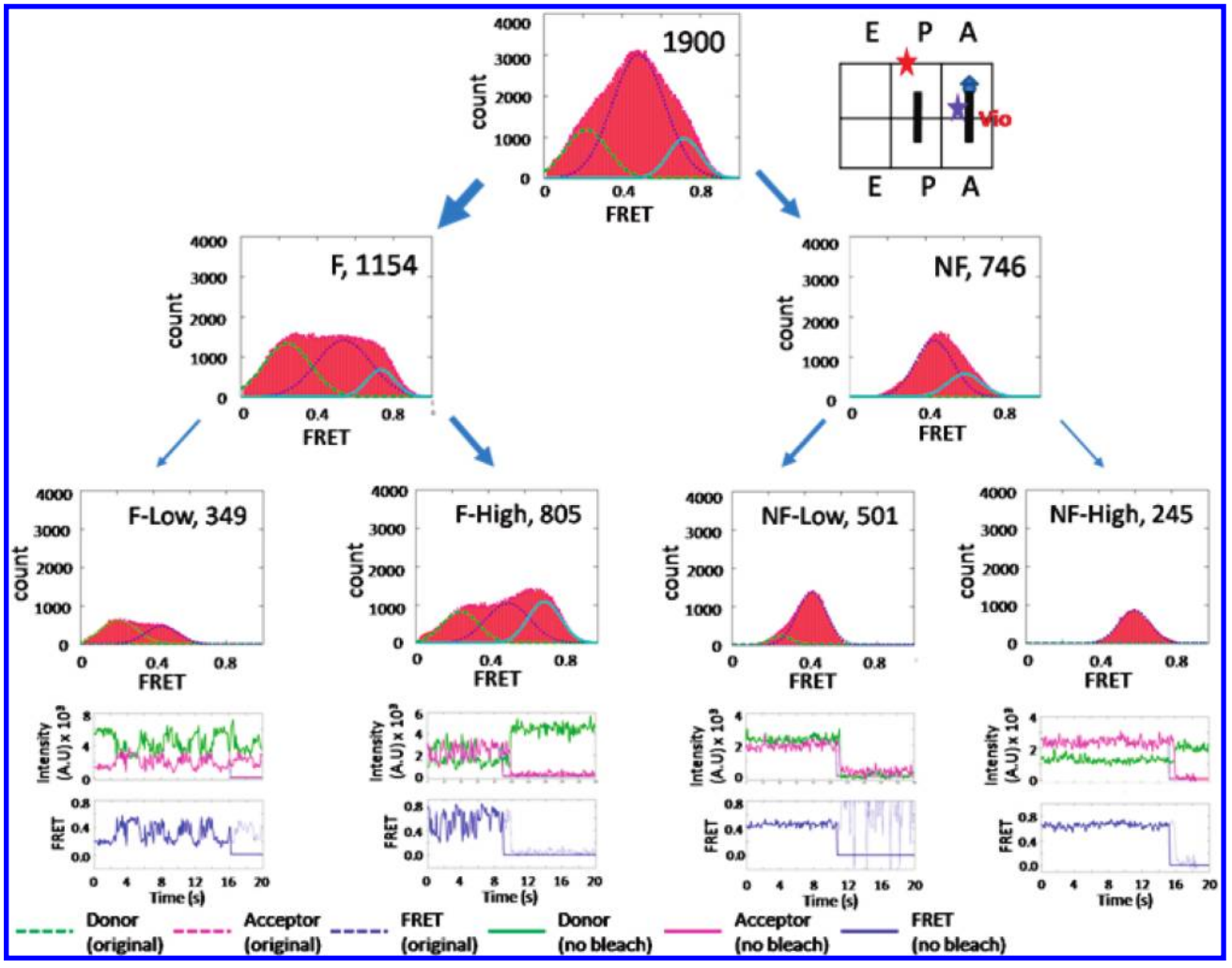

FIGURE 5: Histograms of the pretranslocation complex in the presence of 100 μM viomycin. Four horizontally arranged plots are shown. Details are described in Figure 2.

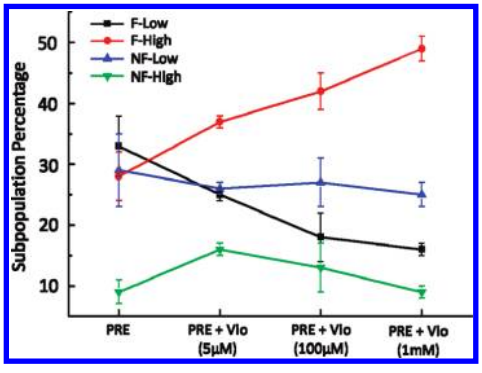

FIGURE 6: The anticorrelated subpopulation changes of F-Low and F-High pretranslocation ribosomes in the presence of various amounts of viomycin. The static ribosomes remained the same.

transition from Hy2 → Hy1 while accelerating the transition from Hy1→ Hy2. Similar deceleration happened in the transition from C→ Hy1 in F-Low subpopulation. A thermodynamic analysis indicated an overall destabilization of the Hy1 by ~0.5 K_BTr and stabilization of the Hy2 by ~0.2 K_BTr, using C as the reference. The rearrangement of the relative energy levels trapped ribosome in the Hy2 state. This observation agreed with the literature reports (*22*, *23*).

Viomycin Induced Instability but Not Back-Translocation in the Posttranslocation Complex. Unlike the pretranslocation experiment, binding of viomycin to the posttranslocation complex redistributed the fluctuating vs nonfluctuating ribosomes. Upon the removal of viomycin, this effect was reversed. Figure 7 shows this process. The terms "posttranslocation complex−100 μM viomycin" and "posttranslocation complex−100 μM viomycin−wash" refer to posttranslocation complexes bound with 100 μM viomycin and the subsequent removal of viomycin by washing. As shown in Figure 7, the locked, stable NF-High subpopulation changed from 69% for the posttranslocation complex (940 particles, Supporting Information Figure S6) to 32% for the posttranslocation complex−100 μM viomycin (1261 particles, Supporting Information Figure S7) and then back to 59% for the posttranslocation complex−100 μM viomycin−wash (2777 particles). Meanwhile, the F-High subpopulation changed from 31% to 68% and then back to 41%. The anticorrelated changes of the NF-High and F-High subpopulations indicated that the binding of viomycin to the stable posttranslocation complex (NF-High) induced unfavorable instability. This instability generated a ribosome distribution profile resembling the pretranslocation complex, implying a possible back-translocation process reported in the literature (*19*). However, three observations opposed this conclusion. First, upon washing away of viomycin, the posttranslocation complex regained its characteristic, stable NF-High subpopulation indicating that this effect was reversible while the back-translocation product should be stable. Second, no significant amount of F-Low

Table 2[a]

		k (s^{-1}), pre complex		k (s^{-1}), pre + 100 μM viomycin		k (s^{-1}), post + 100 μM viomycin
subpopulation	transitions	F-Low	F-High	F-Low	F-High	F-High
F-Low	Hy1 ⇀ C	3.3		2.7		
	C ⇀ Hy1	5.9		3.1		
F-High	Hy1 ⇀ Hy2		4.7		5.7	8.7
	Hy2 ⇀ Hy1		5.2		3.0	4.3

[a]The kinetic fitting of the transitions between Hy1 and C in F-Low subpopulation and between Hy1 and Hy2 in F-High subpopulations. Both the pretranslocation ribosome and that in the presence of 100 μM viomycin were analyzed. The FRET traces are idealized and fitted using the HaMMy analysis package. The dwell time histograms of each FRET state corresponding to specific transitions were then obtained. For example, the transition of Hy1 → C was obtained by counting the dwell times of the FRET state Hy1 before transit into C. Any Hy1 FRET state that transitions into Hy2 was not included and vice versa. The transition rates were then obtained by fitting the dwell time histogram to single exponential decay. Viomycin reversed the relative energy level of Hy1 and Hy2 states and favored the formation of Hy2 state.

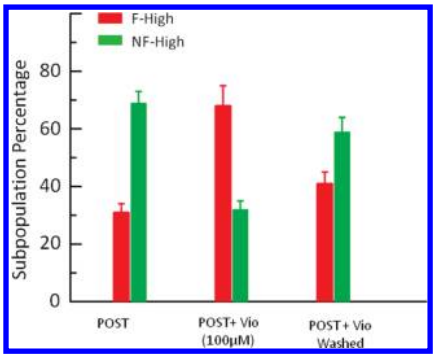

FIGURE 7: The anticorrelated subpopulation changes of NF-High and F-High posttranslocation ribosomes in the presence of 100 μM viomycin. This effect is reversed by washing away the viomycin.

subpopulation was detected in the presence of viomycin, which did not agree with the typical subpopulation distribution of the pretranslocation complex. Third, dynamics of F-High subpopulations in the viomycin-bound posttranslocation complex and pretranslocation complex were dramatically different as shown in Figure 2, Table 2, and Supporting Information Figure S7. Different buffer conditions and mRNA structures may account for the difference in our experiments and those in the literature which reported viomycin-induced back translocation (*19*).

DISCUSSION

Our study indicated that the ribosome pretranslocation complex existed in heterogeneous subpopulations, in agreement with our previous report. We have obtained the following results: (a) the binding of viomycin to the pretranslocation complex induced the F-High subpopulation at the expense of the F-Low subpopulation; (b) kinetic analysis of the F-High subpopulation in the pretranslocation complex indicated that viomycin destabilized the Hy1 state but stabilized the Hy2 state; and (c) the binding of viomycin to the posttranslocation complex induced the F-High subpopulation at the expense of the NF-High subpopulation, and this effect was reversible.

Viomycin Locks the Ribosome at the Ratcheted State. FRET studies directly probing the intersubunit ratcheting showed that viomycin trapped the ribosome at the ratcheted conformation (*14*). A similar single-molecule study supported this conclusion showing that 90% ribosomes were in the ratcheted conformation with negligible fluctuation rate between the unratcheted and ratcheted conformations (*22*). Although our experiments only detected motions of the tRNA acceptor ends, our results were nevertheless consistent with this conclusion.

In our experiments, the static subpopulations of the pretranslocation complex (NF-Low subpopulation) were not affected by viomycin. This result implied that ribosomes with stably bound A/A tRNA were resistant to viomycin binding. Only during ribosome fluctuation can viomycin trap the ribosome in the ratcheted conformation. More ribosome trapped in the ratcheted conformation thus prompted more F-High subpopulation. As shown in Figure 6, the stabilization percentage agreed qualitatively with the previous study (*22*).

However, our experiments showed that the tRNA fluctuations were persistent with viomycin bound (Table 2, Figure 5). Therefore, it is possible to observe either classical (*23*) or hybrid state ribosomes (*24*) in the presence of viomycin. Without subpopulation sorting, the apparent effect of viomycin was to promote more classical state as shown in Figures 2 and 5 and Supporting Information Figure S4 (*23*). On the other hand, in buffers with low Mg^{2+}, hybrid state formation was favored (*24*).

The tRNA Dynamics Are Decoupled with Ribosome Intersubunit Ratcheting. From the study of the tRNA acceptor ends, viomycin was found to induce more F-High population in the pretranslocation complex (Figure 6). This result implied that the fluctuation of tRNA hybrid and classical states was not coupled with the ribosome intersubunit ratcheting, considering literature observations that viomycin trapped the ratcheted ribosome conformation. Kinetic analysis showed that in F-High subpopulation viomycin caused 40% deceleration of Hy2 ⇀ Hy1 and 20% acceleration of Hy1 ⇀ Hy2 transitions. The net effect was that the energy level between Hy2 and Hy1 changed from +0.1 K_BTr to −0.6 K_BTr in favor of Hy2 formation. Compared to viomycin's dramatic inhibition on intersubunit ratcheting (*22*), its effect on tRNA dynamics was modest. Our results implied that viomycin did not inhibit the dynamics in the ribosome peptidyl center, where the tRNA acceptor ends accommodated. With the locked ratcheted conformation, the tRNAs still fluctuated between classical and hybrid states. Therefore, the tRNA dynamics were decoupled with the intersubunit ratcheting. The biologically relevant hybrid state in the cell is probably the synergistic, coincident overlap of the stochastic, uncoupled dynamics of the intersubunit region and the tRNAs.

Two models have been proposed for the dynamic-function relationship of ribosome. In the concerted model, the ribosome intersubunit ratcheting, tRNA P/E-A/P formation, and the closure of L1 protein to interact with P/E tRNA formed the hybrid state in a concerted manner (*25*). However, three-color FRET studies to simultaneously probe dynamics of the tRNAs and L1 protein indicated that these two processes were not coupled. These authors thus proposed that ribosome translocation was via a

multistep stochastic process (*17*). Our studies of viomycin effect implied that the intersubunit ratcheting and the tRNA dynamics were not tightly coupled, in agreement with the multistep model.

Viomycin Disturbed the Stability of the Posttranslocation Complex To Restrain the Translocation Process. We have observed that viomycin prompted fluctuation in the posttranslocation complex but did not promote back-translocation under our experimental conditions. The acylation state of the P-site tRNA determines ribosome dynamics; i.e., acylated tRNA locks ribosome and deacylated tRNA unlocks ribosome for translocation (*10*, *22*). In our experiments, however, viomycin induced fluctuation in the peptidyl-tRNA-locked ribosome conformation. Therefore, it seemed that the viomycin binding pocket at the intersubunit bridge near the decoding site also played an important role in locking the ribosome posttranslocation complex.

We concluded that viomycin probably inhibited translocation by destabilizing the Hy1 state while stabilizing the Hy2 state in the pretranslocation complex and prevented the formation of the stable posttranslocation complex. However, we cannot exclude the possibility that viomycin acts with alternative mechanisms under various conditions. For example, viomycin incubated with the ribosome initiation complex in situ caused more F-High subpopulation in the resulting pretranslocation complex. This result implied that either viomycin bound at alternative pocket or acted differently on different ribosome complexes and conformations.

Finally, the change in ribosome subpopulations in the presence of viomycin demonstrates the biological relevance of our classification of ribosome subpopulations (*26*). Previously, we have reported that more than 80% of ribosomal pretranslocation complexes shifted to nonfluctuate subpopulations when peptidyl-tRNA was replaced with regular acylated or uncharged tRNA at the A-site (*26*). Here, viomycin binding at the intersubunit B2a region shifted the ribosomes toward the F-High subpopulation. These results indicate that the subpopulation interconversions are mainly controlled by distinct chemical changes in the ribosomes rather than ergodic, although about 10% of the ribosomes indeed showed spontaneous transitions among different subpopulations (*26*).

ACKNOWLEDGMENT

We are thankful for the kind gifts of IW312 ribosome glycerol stock from Prof. Robert A. Zimmermann and plasmids from Profs. Yale E. Goldman, Barry S. Cooperman, Rachel Green, and Jacek Wower. We thank Guangtao Song for collecting some single molecule data.

SUPPORTING INFORMATION AVAILABLE

Seven figures to illustrate the FRET labeling strategy, more representative single molecule traces, histograms of FRET efficiency, and kinetic analysis. This material is available free of charge via the Internet at http://pubs.acs.org.

REFERENCES

1. Simonovic, M., and Steitz, T. A. (2009) A structural view on the mechanism of the ribosome-catalyzed peptide bond formation. *Biochim. Biophys. Acta 1789*, 612–623.
2. Schmeing, T. M., and Ramakrishnan, V. (2009) What recent ribosome structures have revealed about the mechanism of translation. *Nature 461*, 1234–1242.
3. Moazed, D., and Noller, H. F. (1989) Intermediate states in the movement of transfer RNA in the ribosome. *Nature 342*, 142–148.
4. Dorner, S., Brunelle, J. L., Sharma, D., and Green, R. (2006) The hybrid state of tRNA binding is an authentic translation elongation intermediate. *Nat. Struct. Mol. Biol. 13*, 234–241.
5. Bretscher, M. S. (1968) Translocation in protein synthesis: a hybrid structure model. *Nature 218*, 675–677.
6. Sharma, D., Southworth, D. R., and Green, R. (2004) EF-G-independent reactivity of a pre-translocation-state ribosome complex with the aminoacyl tRNA substrate puromycin supports an intermediate (hybrid) state of tRNA binding. *RNA 10*, 102–113.
7. Peske, F., Savelsbergh, A., Katunin, V. I., Rodnina, M. V., and Wintermeyer, W. (2004) Conformational changes of the small ribosomal subunit during elongation factor G-dependent tRNA-mRNA translocation. *J. Mol. Biol. 343*, 1183–1194.
8. Semenkov, Y. P., Shapkina, T. G., and Kirillov, S. V. (1992) Puromycin reaction of the A-site bound peptidyl-tRNA. *Biochimie 74*, 411–417.
9. Pan, D., Kirillov, S. V., and Cooperman, B. S. (2007) Kinetically competent intermediates in the translocation step of protein synthesis. *Mol. Cell 25*, 519–529.
10. Valle, M., Zavialov, A., Sengupta, J., Rawat, U., Ehrenberg, M., and Frank, J. (2003) Locking and unlocking of ribosomal motions. *Cell 114*, 123–134.
11. Frank, J., and Agrawal, R. K. (2000) A ratchet-like inter-subunit reorganization of the ribosome during translocation. *Nature 406*, 318–322.
12. Julian, P., Konevega, A. L., Scheres, S. H., Lazaro, M., Gil, D., Wintermeyer, W., Rodnina, M. V., and Valle, M. (2008) Structure of ratcheted ribosomes with tRNAs in hybrid states. *Proc. Natl. Acad. Sci. U.S.A. 105*, 16924–16927.
13. Agirrezabala, X., Lei, J., Brunelle, J. L., Ortiz-Meoz, R. F., Green, R., and Frank, J. (2008) Visualization of the hybrid state of tRNA binding promoted by spontaneous ratcheting of the ribosome. *Mol. Cell 32*, 190–197.
14. Ermolenko, D. N., Spiegel, P. C., Majumdar, Z. K., Hickerson, R. P., Clegg, R. M., and Noller, H. F. (2007) The antibiotic viomycin traps the ribosome in an intermediate state of translocation. *Nat. Struct. Mol. Biol. 14*, 493–497.
15. Frank, J., Gao, H., Sengupta, J., Gao, N., and Taylor, D. J. (2007) The process of mRNA-tRNA translocation. *Proc. Natl. Acad. Sci. U. S.A. 104*, 19671–19678.
16. Horan, L. H., and Noller, H. F. (2007) Intersubunit movement is required for ribosomal translocation. *Proc. Natl. Acad. Sci. U.S.A. 104*, 4881–4885.
17. Munro, J. B., Altman, R. B., Tung, C. S., Cate, J. H., Sanbonmatsu, K. Y., and Blanchard, S. C. (2009) Spontaneous formation of the unlocked state of the ribosome is a multistep process, *Proc. Natl. Acad. Sci. U.S.A.*
18. Modolell, J., and Vazquez (1977) The inhibition of ribosomal translocation by viomycin. *Eur. J. Biochem. 81*, 491–497.
19. Shoji, S., Walker, S. E., and Fredrick, K. (2006) Reverse translocation of tRNA in the ribosome. *Mol. Cell 24*, 931–942.
20. Yamada, T., Mizugichi, Y., Nierhaus, K. H., and Wittmann, H. G. (1978) Resistance to viomycin conferred by RNA of either ribosomal subunit. *Nature 275*, 460–461.
21. Stanley, R. E., Blaha, G., Grodzicki, R. L., Strickler, M. D., and Steitz, T. A. (2010) The structures of the anti-tuberculosis antibiotics viomycin and capreomycin bound to the 70S ribosome. *Nat. Struct. Mol. Biol. 17*, 289–293.
22. Cornish, P. V., Ermolenko, D. N., Noller, H. F., and Ha, T. (2008) Spontaneous intersubunit rotation in single ribosomes. *Mol. Cell 30*, 578–588.
23. Kim, H. D., Puglisi, J. D., and Chu, S. (2007) Fluctuations of transfer RNAs between classical and hybrid states. *Biophys. J. 93*, 3575–3582.
24. Feldman, M. B., Terry, D. S., Altman, R. B., and Blanchard, S. C. (2010) Aminoglycoside activity observed on single pre-translocation ribosome complexes. *Nat. Chem. Biol. 6*, 244.
25. Frank, J., and Gonzalez, R. L., Jr. (2010) Structure and dynamics of a processive Brownian motor: the translating ribosome, *Annu. Rev. Biochem.*
26. Altuntop, M. E., Ly, C. T., and Wang, Y. (2010) A single molecule study of ribosome's hierarchic dynamics at the peptidyl transferase center, *Biophys. J.* (in press).
27. Wang, Y., Qin, H., Kudaravalli, R. D., Kirillov, S. V., Dempsey, G. T., Pan, D., Cooperman, B. S., and Goldman, Y. E. (2007) Single-molecule structural dynamics of EF-G−ribosome interaction during translocation. *Biochemistry 46*, 10767–10775.
28. Rasnik, I., McKinney, S. A., and Ha, T. (2006) Nonblinking and long-lasting single-molecule fluorescence imaging. *Nat. Methods 3*, 891–893.
29. McKinney, S. A., Joo, C., and Ha, T. (2006) Analysis of single-molecule FRET trajectories using hidden Markov modeling. *Biophys. J. 91*, 1941–1951.
30. Fei, J., Kosuri, P., MacDougall, D. D., and Gonzalez, R. L., Jr. (2008) Coupling of ribosomal L1 stalk and tRNA dynamics during translation elongation. *Mol. Cell 30*, 348–359.